A Comparative Study of Quasi-solid Nanoclay Gel Electrolyte and Liquid Electrolyte Dye Sensitized Solar Cells

by

Laura Main

A Thesis Presented in Partial Fulfillment
of the Requirements for the Degree
Master of Science in Technology

Approved November 2012 by the
Graduate Supervisory Committee:

Lakshmi Munukutla, Chair
Arunachalanadar Madakannan
Gerald Polesky

ARIZONA STATE UNIVERSITY

December 2012

ABSTRACT

Dye sensitized solar cells (DSSCs) are currently being explored as a cheaper alternative to the more common silicon (Si) solar cell technology. In addition to the cost advantages, DSSCs show good performance in low light conditions and are not sensitive to varying angles of incident light like traditional Si cells.

One of the major challenges facing DSSCs is loss of the liquid electrolyte, through evaporation or leakage, which lowers stability and leads to increased degradation. Current research with solid-state and quasi-solid DSSCs has shown success regarding a reduction of electrolyte loss, but at a cost of lower conversion efficiency output. The research work presented in this paper focuses on the effects of using nanoclay material as a gelator in the electrolyte of the DSSC.

The data showed that the quasi-solid cells are more stable than their liquid electrolyte counterparts, and achieved equal or better I-V characteristics. The quasi-solid cells were fabricated with a gel electrolyte that was prepared by adding 7 wt% of Nanoclay, Nanomer® (1.31PS, montmorillonite clay surface modified with 15-35% octadecylamine and 0.5-5 wt% aminopropyltriethoxysilane, Aldrich) to the iodide/triiodide liquid electrolyte, (Iodolyte AN-50, Solaronix).

Various gel concentrations were tested in order to find the optimal ratio of nanoclay to liquid. The gel electrolyte made with 7 wt% nanoclay was more viscous, but still thin enough to allow injection with a standard

syringe. Batches of cells were fabricated with both liquid and gel electrolyte and were evaluated at STC conditions (25℃, 100 mW/cm ^{2}) over time. The gel cells achieved efficiencies as high as 9.18% compared to the 9.65% achieved by the liquid cells. After 10 days, the liquid cell decreased to 1.75%, less than 20% of its maximum efficiency. By contrast, the gel cell's efficiency increased for two weeks, and did not decrease to 20% of maximum efficiency until 45 days. After several measurements, the liquid cells showed visible signs of leakage through the sealant, whereas the gel cells did not. This resistance to leakage likely contributed to the improved performance of the quasi-solid cells over time, and is a significant advantage over liquid electrolyte DSSCs.

DEDICATION

This and everything else in my life is for my son, Nathan.

I love you.

ACKNOWLEDGMENTS

I would first off like to thank Dr. Lakshmi Munukutla for giving me the wonderful opportunity to work under her guidance and with her continued support throughout this research project. Without her, none of this would have been possible, and I am grateful to her for that.

Dr. Arunachalanadar Madakannan was instrumental during this project, and a big thanks goes to him as well for his much appreciated wisdom and advice.

I am also grateful to the other professors and staff who provided support and assistance during my time at ASU Polytechnic, notably Dr. Govindasamy Tamizhmani, Dr. Gerald Polesky, and especially Martha Benton and Julie Barnes who always came through for me to ensure all I's were dotted, and all T's were crossed.

I am indebted to my fellow students Brian Fauss and Travis Curtis who put in so much hard work on this project and helped work through the many speed bumps we faced along the way. I know they will be successful in all that they do in life, and I wish them nothing but the best.

Finally, there are no words to describe the gratitude and love I feel for my family who have really gone to extremes to support me through this Masters program. The tremendous amount of time spent on this research project was time not spent with my husband and new son, but they never complained. Nathan and Joe, this accomplishment is as much yours as it

is mine, I love you. Mom, I can't ever pay you back for what you've done, taking care of the most important thing in the world to me so that I could focus on reaching my goals, thank you.

TABLE OF CONTENTS

Page

CHAPTER Page

LIST OF TABLES

LIST OF FIGURES

Figure Page

Chapter 1

INTRODUCTION

1.1 Purpose

The most common source of energy today is derived from fossil fuels. While this type of fuel has been an abundant resource since the industrial revolution, domestic oil production is now decreasing [1]. This creates an urgent need for alternative energy sources.

While unconventional oil such as oil sands and oil shale supplies are still available, the recovery and processing of these fuels have many negative environmental impacts including increased emissions, high levels of water usage, and groundwater contamination [1]. The increased CO_2 emissions produced when recovering unconventional oil is enough reason to render this a less than ideal option as an alternative energy source. The Inter-governmental Panel on Climate Change (IPCC) reported in 2007 that the averaged global surface temperature may increase as much as 6.4℃ by the year 2100 if nothing is done to reduce our carbon emissions [2]. However, within the international scientific community, the generally accepted danger limit is perceived to be 2℃ above pre industrial temperatures, which is only 1℃ higher than today. An International Energy Agency (IEA) report released in 2011 states that the global CO_2 emissions increased 3.2% from 2010 and projections for 2012 are not much better. In order to address the rising averaged global surface temperature, it is critical that our world begins to transition to renewable

energy sources with low to no CO_2 emissions, and solar energy is the most viable option to reach this goal.

1.2 Background

Solar technology converts energy from the sun into electricity. A solar cell can produce electricity without any toxic by-products, and most importantly, no CO_2 emissions over several decades, utilizing the sun as an abundant renewable source of energy. One of the major factors currently limiting the expansion of the solar industry is the high initial cost of producing the cells. Some of the semi conductor materials used in traditional solar cell fabrication, like silicon (Si), cadmium (Cd), and tellurium (Te), are expensive. There are other solar technologies emerging such as dye sensitized solar cells (DSSCs), which do not require the expensive semiconductor material used in traditional solar cells, and have the potential to make solar technology affordable for the average consumer.

A typical DSSC consists of two electrodes, comprised of conductive glass, sandwiched together and filled with an electrolyte material as shown in Figure 1. The working electrode, also known as the anode, is coated with a layer of titanium dioxide (TiO_2) semiconducting material. The electrode is then soaked in a charge transfer dye, known as the sensitizer, which is adsorbed by the TiO_2 nanoparticles. The electrode performs the function of absorbing the light and transferring that energy into an electron, which can be used by an external circuit. The counter

electrode glass is coated with a thin layer of catalyst material, typically platinum (Pt). This electrode delivers an electron from the external circuit back into the cell. In between the two electrodes, a gasket is used to create a small cavity, which is filled with the electrolyte material, generally based on an iodide/triiodide redox couple (I^-/I_3^-). The electrolyte serves as the charge carrier between the two electrodes, which is discussed in more detail in chapter 2. This process is very similar to the natural process of photosynthesis that occurs every day all around us. The main difference is that instead of light being converted into energy for the plants to survive, with DSSCs it is converted to electricity.

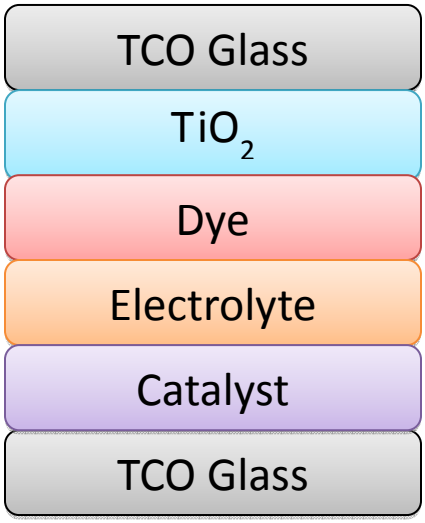

Figure 1: Basic Layered Device Architecture of a DSSC

The DSSC technology offers many benefits over other solar cell technologies including environmental impact, cost, and behavior in non-ideal settings. Toxicity is a major issue when it comes to solar cell production. There have been concerns that the production, use and

disposal of solar panels may have a harmful impact to the environment. The arsenic and cadmium used in the high efficiency cells described above are toxic materials. In standard high efficiency PV technology, these harmful materials such as telluride and arsenide are used. However, TiO_2 is non-toxic, safe enough to be used in nutritional supplements consumed by humans. The DSCC fabrication methodology is very simple and the waste generated is far less than compared to the matured silicon solar technology.

The simple process, coupled with inexpensive raw materials, results in a much lower fabrication cost estimated at about 20-30% of the cost it takes to fabricate traditional Si solar cells. While the technology is fairly new it is difficult to get good data to project the cost of DSSC and has not been commercially produced long enough to gather good data. However, rough estimates show the cost of DSSC is around \$48-64/m^2 and less than \$ 1 per peak watt and may even come down to as low as \$0.48 W_p [3]. This is much cheaper than CdTe cells, which are estimated to cost about \$130/m^2 and \$1.65 W_p [4].

TiO_2, the most commonly used semiconductor material in DSSCs, provides many advantages over the materials used in p-n junction cells. In fact, most of the materials used in DSSC manufacturing are very inexpensive, which adds to the lower cost when compared to traditional Si solar cells. TiO_2 is readily available compared to silicon, which has to be grown from crystals is a very time consuming process, especially for pure

single crystal Si. Gallium arsenide (GaAs) and cadmium telluride (CaTe) p-n solar cells are high in efficiency, but gallium and tellurium are very rare materials, which results in a much higher cost. TiO_2 on the other hand, is abundant enough that it is used in common household products like toothpaste, sunscreen, and paint pigmentation.

When looking at many practical applications of solar technology such as building integrated photovoltaics (BIPV) and indoor use, DSSCs significantly outperform traditional Si based solar cells. This is because DSSCs accept smaller angles of incident light, are less sensitive to fluctuations in irradiance, and can withstand greater temperature ranges. When panels were placed 90° from horizontal and tes ted at various sun positions, the DSSCs exhibited 20-60% increase in performance over Si modules [5]. Unlike traditional Si cells, which can experience significant drops in performance without full sun, DSSCs perform well and produce power under shade and with cloudy skies. Most commercial panels are rated at 25℃, but temperatures outside of the labo ratory are usually higher, which results in a performance drop at the consumer level. With DSSCs, the temperature increase has a much smaller effect, which offers a significant advantage for the consumer. An increase from 20℃ to 50℃ results in a 19.5% max power (P_{max}) drop for c-Si panels, but only a 5% max power drop for DSSC panels [5].

There are challenges facing the DSSC technology that need to be overcome in order to make it competitive with Si modules. One major

issue is the lower energy conversion efficiency output compared to standard Si cells. While DSSCs are now showing results similar to amorphous silicon cells, they have yet to achieve the high efficiency output of c-Si cells. There are several components of the DSSC that have the potential to improve the efficiency of the light to power conversion, such as material used for the anode, cathode, and electrolyte, as well as the fabrication procedure itself.

One of the major challenges facing DSSCs is leakage of the liquid electrolyte, which lowers stability and leads to increased degradation. This can occur during fabrication or simply with prolonged exposure to the sun. During fabrication, if the cell is not completely sealed, there can be leaks, which quickly drain the cell's efficiency. Even with a successfully sealed cell, liquid electrolyte material will eventually be evaporated when exposed to the sun, and will need to be replenished periodically to maintain its high efficiency. To circumvent this challenge, earlier research work attempted to fabricate the DSSCs with non liquid electrolyte material, but significant decrease in efficiencies of up to 60% was observed.

1.3 Scope

This thesis project will examine alternatives to liquid electrolyte material, specifically quasi-solid electrolyte, to see if its application can solve the problems observed with liquid electrolytes, without sacrificing the efficiency. The intent of this paper is to present information obtained via research and experimentation regarding the performance of quasi-solid dye sensitized solar cells fabricated in a laboratory environment. It will deal with the experimental setup, the various materials used, and the performance results. Chapter 2 provides a review of the most relevant literature regarding alternatives to liquid electrolyte material. The fabrication process as well as testing methods will be covered in Chapter 3. The experimental results are presented in Chapter 4, as well as an analysis of the data. Chapter 5 summarizes the experimental results and states final conclusions for the project as well as suggestions for further research.

Chapter 2

LITERATURE REVIEW

While the fundamental electrochemical process has been used in photography since the beginning of the 19th century, studies of the electron transfer process of a semiconductor oxide material picked up much later in the 1960s. These cells consisted of single crystal TiO_2 surrounded by chlorophyll, which resulted in less than 1% efficiency. This design was improved upon by using smaller 20 nm nanoparticles of the TiO_2 semiconductor, which increased the surface area thereby increasing the amount of electrons transferred. A sensitizing dye material replaced the chlorophyll, which was able to quickly inject electrons when excited by sunlight. With more absorption and surface area for the transfer of electrons, the efficiency increased significantly. In 1991 Michael Grätzel and Brian O'Regan first introduced DSSCs as we now know them, with a conversion efficiency of 7.1% [6]. Since that time, new innovations with materials and design processes have resulted in a recorded efficiency of 12.3%, from a cell using a porphyrin dye and a $Co^{(II/III)}$tris(bipyridyl)-based redox electrolyte [7]. DSSCs were introduced to the market globally in 2007, with companies like Sony, 3G, and G24 Innovations being a few of the key market players. Now that cells are being produced that have efficiencies higher than some amorphous silicon cells, there is great potential for the DSSC market to expand even further.

2.1 Fundamental Operation

DSSCs are different than traditional p-n junction cells in that they separate the light absorption and charge carrier transport functions, whereas the semi conductor material does both in traditional photovoltaic cells.

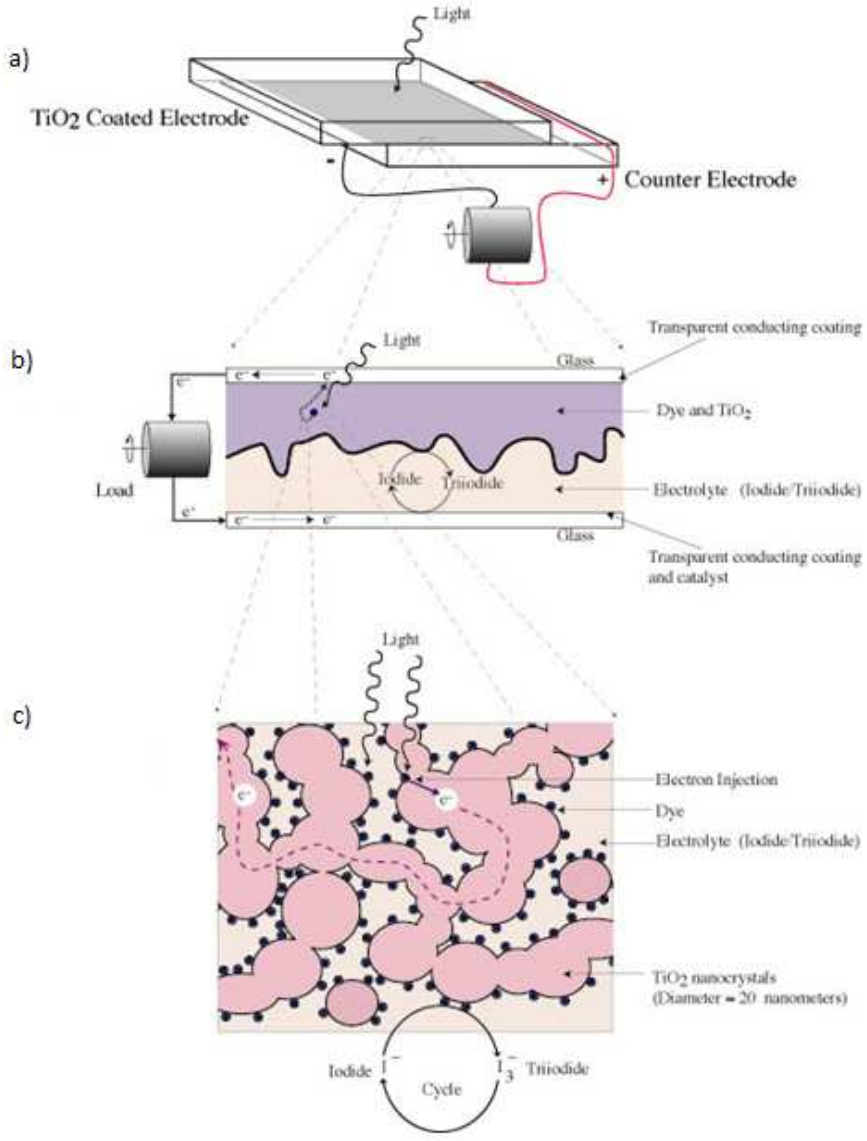

Figure 1: DSSC structure (a) Electrodes in circuit; (b) Cross sectional view of cell; (c) Enhanced view of TiO_2/dye/electrolyte interface

Figure 1a-c breaks down the DSSC structure starting with a simplified view of the cell, highlighting the working electrode, which is coated with the TiO_2 and is the electrode exposed to light, and the counter electrode, which is coated with the catalyst material, usually platinum (Pt). Figure 1b depicts the view of the electrolyte filled gap between electrodes, and the electron flow from working electrode to external circuit back to the counter electrode. The image is further magnified in Figure 1c to show the TiO_2 nanoparticles coated with the dye, which is surrounded by the iodide/triiodide (I^-/I_3^-) redox couple electrolyte material. When the dye absorbs photons from the sun, it becomes photo excited, and injects an electron into the conduction band of the TiO_2. Within the electrolyte a redox reaction takes place at the working electrode, which donates an electron to the dye, and at the cathode, the triiodide (I_3^-) accepts an electron from the Pt coated conductive glass, a reduction reaction takes place regenerating the redox couple, and the cycle is completed without causing permanent chemical transformation of any material involved.

2.2 Role of the Electrolyte

The electrolyte facilitates two important tasks in the DSSC process. It serves as the transport mechanism for the redox mediator from the TiO_2 electrode to the counter electrode where electron transfer will occur and the triiodide ions will be reduced to iodide as shown by the following reaction:

$$I_3^- + 2e^- \rightarrow 3I^-$$

Because there are no minority charge carriers involved, the bulk recombination losses normally associated with lattice defects in Si based solar cells do not occur in DSSCs [6]. At the TiO_2 side, the electrolyte serves to regenerate the dye molecule, which has been oxidized following the electron injection into the conduction band of the TiO_2. This regeneration is represented by the following reaction:

$$3I^- \rightarrow I_3^- + 2e^-$$

This is very important because it prevents the dye molecule from being reduced via recombination of a TiO_2 electron. There are two methods of recombination of TiO_2 electrons. One is with the oxidized dye molecules, but this is unlikely because the regeneration from the iodide is very fast. The second more likely method is recombination of the electrons in the TiO_2 with the acceptors in the electrolyte. The electron lifetime refers to the recombination of the TiO_2 electrons with electrolyte acceptors. The iodide/triiodide redox couple exhibits longer (1-20 ms) lifetimes than other redox couples that have been tried before, for example cobalt-based and organic systems, and that is why it remains the preferred electrolyte material [8]. For this reason, the I^-/I_3^- redox couple was used as the basis for the quasi-solid electrolyte tested in the experiments discussed in this paper.

2.3 Electrolyte Requirements

There are several characteristics that an electrolyte must exhibit in order to achieve good performance from the DSSC. In addition to serving

as a solvent for the redox couple, it must be chemically stable so that it doesn't have any unintended reactions with any of the other materials in the cell including the sealant. It shouldn't absorb light as this would result in filtering effects. In order for the dye regeneration to occur, the difference between the oxidation potential of the dye and the redox potential of the electrolyte, given as (ΔG^0), has to be sufficient. For a typical ruthenium (Ru) based dye and a standard I^-/I_3^- electrolyte, the driving force is given by $\Delta G^0 = 0.75$ eV. The following example shows how this is calculated:

Oxidation potential of dye, $Ru(dcbpy)_2(NCS)_2 = +1.10$ V

Redox potential of I^-/I_3^- electrolyte = +0.35 V

Therefore, $\Delta G^0 = 1.10 \text{ V} - 0.35 \text{ V} = 0.75$ eV

Based on experimentation of different dye chemistry, it was found that using osmium (Os) instead of Ru resulted in $\Delta G^0 = 0.54$ eV, that causes slow regeneration [9]. However, black dye, $Ru(tcterpy)(NCS)_3$, results in $\Delta G^0 = 0.6$ eV, and exhibits high regeneration rate [10]. This driving force must be taken into account when choosing an electrolyte material, because if the redox potential is too high, the driving force is reduced, and if it falls much lower than 0.6 eV, the performance of the DSSC will be greatly reduced. Ionic conductivity is also important in electrolyte material and it must be high so that the electron transfer can occur at the electrodes fast enough to keep up with the electron injection of the dye, and do so with negligible ohmic loss. This generally means that the

electrolyte must be highly viscous, which is why liquid electrolyte material is most commonly used. However, there are drawbacks to using liquid as the electrolyte material such as desorption of the dye, corrosion of the Pt, overall stability, and leakage of the electrolyte itself.

2.4 Drawbacks of Liquid Electrolyte

Liquid electrolyte cells struggle to meet the rigorous reliability testing required to become commercially viable because the liquid material because they often fail to meet the long term stability requirements at temperatures above 80℃ as seen in Figure 2: Evolution of: (a) current-density vs. time; (b) open-circuit voltage vs. time; (c) and the efficiency vs. time [11]Figure 2. This figure shows how current and efficiency are greatly affected by higher temperatures, though open circuit voltage (V_{OC}) is only slightly reduced. The decrease in current was attributed to degradation of the dye material and to a loss of electrolyte via evaporation or leakage [11].

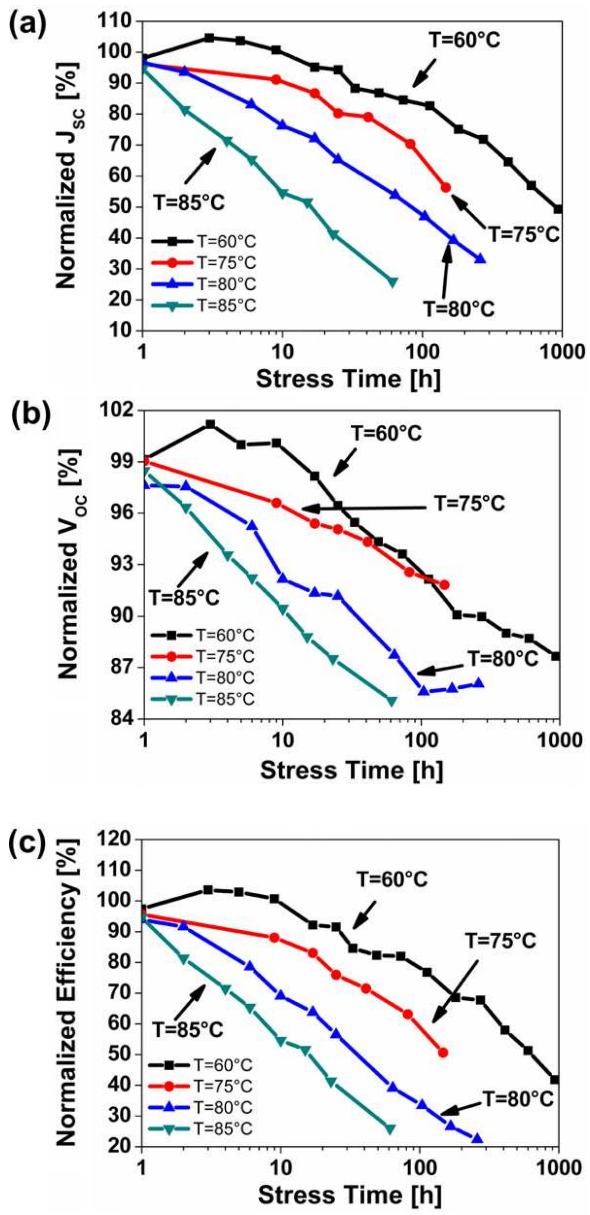

Figure 2: Evolution of: (a) current-density vs. time; (b) open-circuit voltage vs. time; (c) and the efficiency vs. time [11]

Evaporation and leakage is a major problem facing DSSCs with liquid electrolyte material. If the cell is not perfectly sealed, the electrolyte material will escape through evaporation, which will cause the cell to degrade. This requires careful sealing methods during fabrication, which

can increase fabrication time and costs. Even cells that are sealed perfectly may experience evaporation of the electrolyte material over time, as the sealant wears out due to environmental factors like temperature and internal factors like reactions with electrolyte material.

2.5 Other Electrolyte Possibilities

Solid state DSSCs using hole transport material (HTM) offer an alternative to using liquid electrolyte and do not suffer many of the drawbacks like leakage, desorption, and corrosion. P-type solid semiconductor material has been used as a HTM in solid state DSSCs with recorded efficiencies of 3.8% for a cell using Cu (I) [12]. However, in addition to having much lower conversion efficiency than its liquid electrolyte counterpart, the stability of the solid state DSSC remains an issue, as it does with most inorganic HTMs. This brought focus to organic HTMs, which initially showed efficiencies less than 1%, but through more experimentation like that of Cai *et al*, now have recorded efficiency values of 6.08% using organic hole transporter spiro-MeOTAD [13]. While this is a significant improvement over the Cu(I) efficiency value, it still remains lower than DSSCs using liquid electrolyte because HTMs have lower intrinsic conductivity, experience higher recombination rates with TiO_2 electrons, and don't penetrate as well into the dye as liquid electrolyte does [12].

The other liquid electrolyte alternative currently gaining attention is quasi-solid DSSCs, which use gel electrolyte material usually based on a

redox couple similar to liquid DSSCs. Quasi-solid cells also offer solutions to the problems facing liquid electrolyte cells, but have an even greater advantage in that they have shown greater stability. Similar to solid-state DSSCs, a common drawback with quasi-solid electrolyte material has been a decrease in the efficiency due to higher viscosity, which results in a restriction of ionic mobility. Different materials have been researched as possible gelators in quasi-solid cells, even common household items like SuperGlue®, which was mixed with a triiodide/iodide redox couple, and successfully produced DSSCs with efficiencies of 4% [14]. Polymer electrolytes are a popular quasi-solid material, but at lower temperature, the polyethylene oxide (PEO) solvent crystallizes, which decreases conductivity and lowers efficiency output [15]. This led to research into using inorganic fillers to improve the low conductivity of the PEO. Meneghetti *et al* used high molecular weight polymethymethacrylate (PMMA) and montmorillonite (MMT) clay to create a polymer nanocomposite gel electrolyte that increased conductivity from 7.6×10^{-4} S/cm^2 to 9.1×10^{-4} S/cm^2 [16].

DSSCs already have lower efficiency output than many Si solar cells; therefore, it is very important to find a method of gelling the electrolyte to increase stability without compromising any of its performance characteristics. Researchers are now attempting to improve on the efficiency of DSSCs using quasi-solid electrolytes. Yu *et al* used a cyclohexanecarboxylic acid-[4-(3-octade-cylureido)phenyl]amide-based

gel electrolyte with Ru dye C105 to achieve quasi-solid cell efficiency of 9.1% that shows stability at 60℃ [17]. Grätzel *et al* were able to show that using fumed silica nanoparticles, mixed with an MPII-based electrolyte, allowed the electrolyte to penetrate the TiO_2 layer, resulting in efficiencies matching the corresponding liquid electrolyte cells [18].

This paper documents research work done with a quasi-solid DSSC made from MMT clay and an iodide based high viscosity electrolyte, in an effort to compare the performance characteristics and stability over time with liquid electrolyte DSSCs. The following chapter details the evolution of the DSSC fabrication process, and the reasoning behind changes that were made. The methods utilized to test and evaluate the cells are also presented in Chapter 3.

Chapter 3

EXPERIMENTAL METHODS

The fabrication of a DSSC can have a great impact on the performance of the cell. The materials used as well as the fabrication procedure are critical to ensuring a cell that not only performs well, but also sustains consistent performance. Therefore, various materials and methods were experimented with, and the resulting cell performance was evaluated. Many improvements were made to the original process, resulting in a refined, efficient fabrication process, using the best suited materials. Testing methods were also evaluated and adjusted in an attempt to minimize unwanted variables and obtain accurate results. The following sections describe the fabrication procedures of the DSSCs, provide information about the materials used, and the detailed testing methods employed.

3.1 Fabrication Procedures of DSSC

The fabrication procedure of the DSSCs consisted of 9 steps, completed over three (3) days as shown in Figure 3. On the first day, the electrodes are coated with TiO_2 material and then sintered overnight. The following day, the counter electrode is coated with Pt and then sintered overnight, and the TiO_2 electrodes are soaked overnight in the dye. The third day, the two electrodes are assembled, the cell is filled with electrolyte, and then it is sealed.

There was also preparation that had to be done prior to fabrication. This included preparing the substrates, cutting the sealant, and mixing the dye and gelled electrolyte material. These processes as well as the fabrication steps are described in detail below.

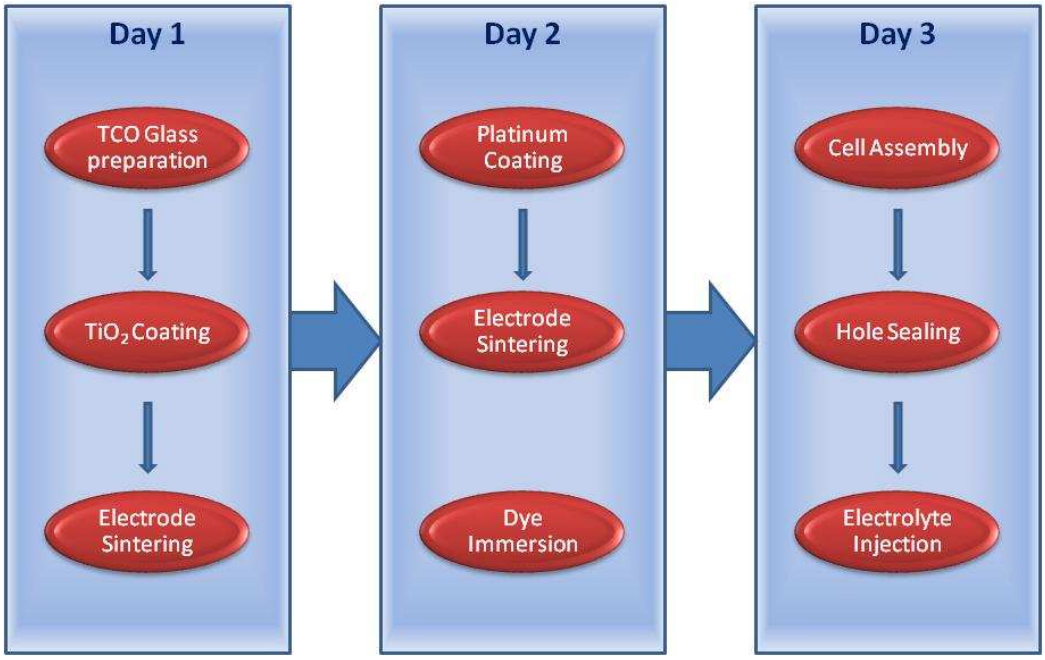

Figure 3: Fabrication Procedures of DSSC

3.1.1 Glass Substrate Preparation

The substrate used for the DSSC electrodes was a 2mm thick, transparent conducting oxide coated (TCO) glass, (TCO22-7, Solaronix), coated with a fluorine doped tin oxide (FTO) layer. Each 5 cm x 5 cm piece of glass was cut into smaller pieces in order to reduce the sheet resistance, thereby improving efficiency. Using a cutting/engraving laser machine, (Universal Laser Systems), 16 pieces of 13 mm x 13 mm were cut from each sheet of glass. Originally, the glass was cut in several stages, which required lifting & replacing pieces off the metal tray, which

sometimes led to scratches on the conductive coating. To reduce scratching, a template was created and a program written for the laser machine software, which made all of the cuts without ever having to move the glass.

Figure 4 shows how the smaller electrodes are made from the larger piece of glass after the laser program has been run. The time required to make 16 pieces of glass was greatly reduced and the quality of those pieces increased, resulting in less wasted material.

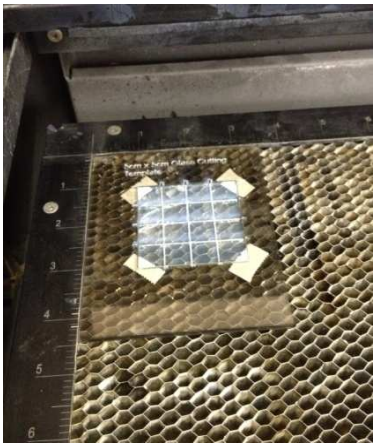

Figure 4: TCO glass electrodes cut from 5 cm^2 piece of glass

The counter electrode was drilled with a single hole for liquid electrolyte filling and two holes for gel electrolyte filling. Using two holes was necessary for the gel because the increased viscosity made it difficult to use the vacuum plunger that was used with liquid electrolyte. A syringe was used to inject the gel electrolyte, so the second hole provided a vent for air, which prevented air bubbles and ensured the gap was completely filled with electrolyte. The drill bit size was reduced to 0.45 mm in order to prevent Pt from draining during application and electrolyte from draining out after final assembly.

3.1.2 TiO_2 Active Area

The working electrode was coated with a 100µm layer of TiO_2 (Ti-Nanoxide D, 15-20 nm, Solaronix) using the Coatema® Easy Coat machine with a precision doctor blade attached. Originally, a glass rod was attached to the Coatema tool, but it was very difficult to accurately calibrate the rod over the entire surface of the template. Therefore, the rod was replaced by the blade, which produced even TiO_2 layers that were consistently repeatable.

A mask was created by cutting a 7mm x 7mm square out of 3 layers of Scotch® Magic™ Tape applied to a template, which was created using a thickness equal to that of the glass substrate. The automated laser machine was used to make the electrode cuts, which ensured identical active areas for every cell.

The pieces of glass are then cleaned with isopropyl alcohol (IPA) and placed under the mask, which was firmly adhered to the FTO layer with slight pressure. The plastic template consisting of four masked substrates was then placed on the Coatema tool in a calibrated position as shown in Figure 5a. The height of the blade was calibrated by placing a 0.04 mm shim between a precise location on the plastic template and the blade. This calibration method was tested repeatedly, and the resulting layers were examined under a microscope until all four cells in the template displayed uniformly thin layers. To ensure consistency, the calibration was performed prior to each coating.

a) 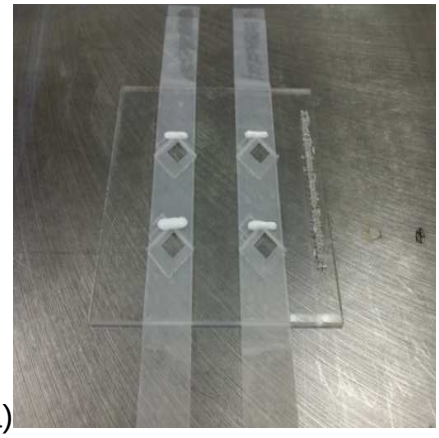 b) 

c) 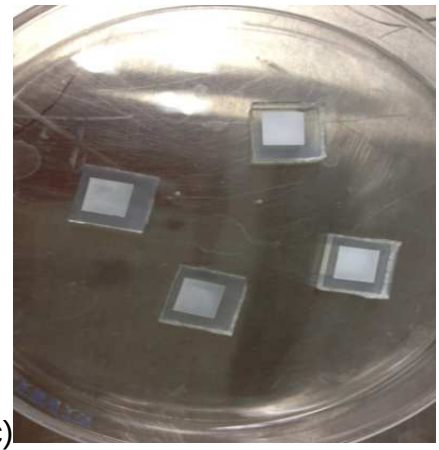

Figure 5: Working electrode coating process (a) Substrate prior to coating; (b) Coated TiO_2 layers; (c) TiO_2 electrodes prior to assembly

The TiO_2 material was then applied to the mask and the blade was moved slowly across the template resulting in an even consistent thickness of TiO_2 active area as shown in Figure 5b. The electrodes were immediately covered with Petri dishes to prevent any impurities and allowed to dry. The masks were then removed and the electrodes are sintered for 1 hour at 400℃ and then left in the o ven to cool overnight. The following day, the electrodes were removed from the oven and placed in the Ru dye, Ru(II)L2(NCS)2 : 2 TBA (tetrabutyl ammonium) (L=2, 2′-bipyridyl-4, 4′-dicarboxylate, N719, Solaronix) with ethanol solution, where they were left to soak for a minimum of 12 hours. At the end of these operations, the completed working electrodes were obtained as shown in Figure 5c.

The initial calibration procedure was highly dependent on the person performing the calibration, which resulted in inconsistent thickness from one batch to the next. Also, the template was wide enough that the height of the cell on one side was not the same as that on the other side, which also resulted in layers that were too thick causing cracking, depicted in Figure 6a. Modifying the template and positioning it in the same place on the Coatema machine each time, as well as developing an accurate repeatable calibration method improved the TiO_2 layers as shown in Figure 6b.

a) 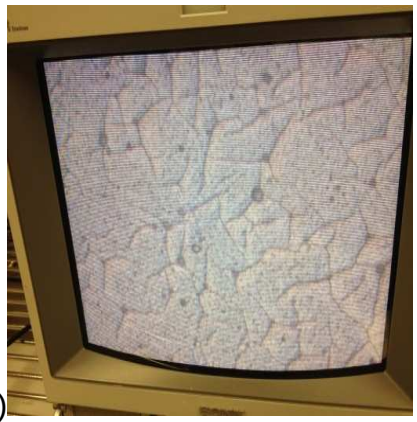 b) 

Figure 6: TiO_2 coating as seen at 10x magnification

(a) cracking of thicker layer; (b) thin even layer

3.1.3 Platinum Counter Electrode

The counter electrode was coated with a Pt catalyst layer (Platisol T/SP, Solaronix). The Pt coating was done by hand using the doctor blade technique as shown in Figure 7a, and only two layers of tape were used resulting in about a 67µm layer of Pt. Similar to the TiO_2 procedure, the Pt electrodes were immediately covered with Petri dishes, dried, and sintered for 1 hour at 400℃, remaining in the oven to cool overnight. The result was the counter electrode, ready for assembly as shown in Figure 7b.

a) 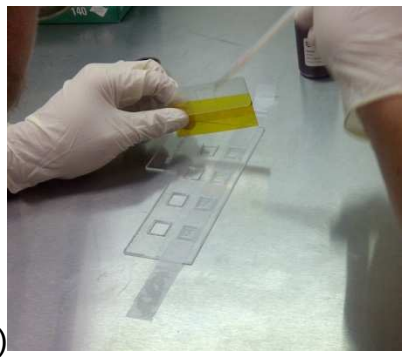 b) 

Figure 7: Counter electrode (a) during Pt application;

(b) Pt layer after sintering

3.1.4 Cell Assembly

The most critical part of cell fabrication is the assembly, and so a good amount of effort went into this part of the process. Cell assembly consists of 3 steps; sealing the two electrodes, injecting the electrolyte, and then sealing the injection hole. Sealant material is cut in masks of 5.5 mm x 5.5 mm to lie just inside the active area as shown in Figure 8a. Various methods of sealant cutting were tried first, including using a scalpel, which was hard to control, the laser machine, which was too hot, and finally the punch blade, which produced the best results. The sealant material was also changed from a 25 µm thick Surlyn® sealant, (Meltonix, 1170-25, Solaronix) to a 60 µm thick Bynel® sealant, (Meltonix, 1162-60, Solaronix), because the increased thickness made the sealing more consistent around the active area of the cell. The sealant is then sandwiched between the two electrodes, which has to be carefully placed so that the active areas are aligned correctly as shown in Figure 8b.

a) 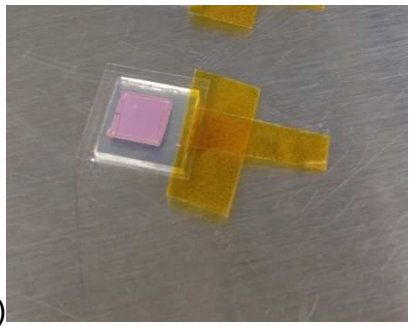 b) 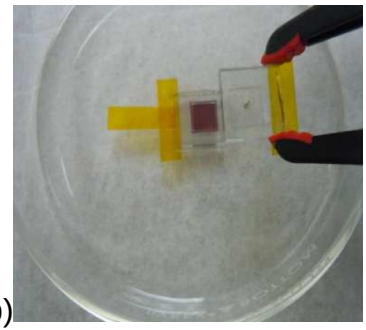

Figure 8: Cell assembly a) sealant on working electrode;

b) Counter electrode placement

Originally, binder clips were used to hold the electrodes together while the sealant melted, however this allowed for a significant risk of human error as the electrodes tended to shift during placement of the binder clips. A specially designed press shown in Figure 9a replaced the binder clips and automated the trickiest part of the sealing process. However, over time the press material warped, resulting in an uneven sealing of the cells and subsequent electrolyte leaking. In order to control the sealing better, a hot plate, heated to about 140℃, was used to heat the sealant, and pressure was manually applied continuously for about 5 minutes or until it was observed that the sealant had evenly melted and adhered to the electrodes. This process is illustrated in Figure 9b.

a) 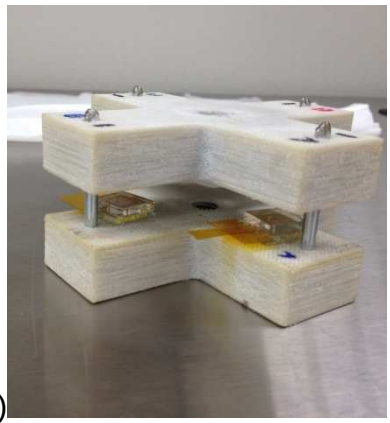 b) 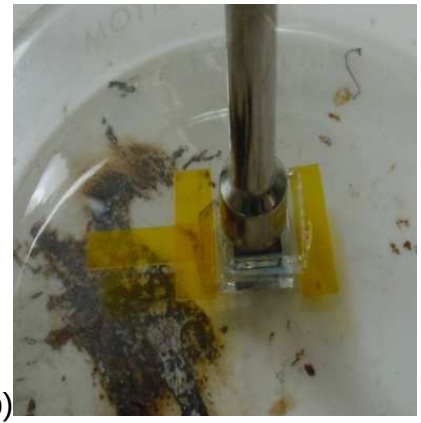

Figure 9: Sealing process using (a) assembly press; (b) hot plate

3.1.5 Liquid Electrolyte Injection

After the two electrodes were sealed together, the liquid electrolyte, (Iodolyte AN-50, Solaronix) was injected by using the vacuum plunger as shown in Figure 10a. Initially a syringe was used to inject the electrolyte, but this method made it difficult to eliminate all the air bubbles. There was

also the risk of the needle making contact with the working electrode, which reduced conversion efficiency due to a damaged TiO_2 layer. The plunger had the added advantage of greatly reducing waste, because only the needed amount of electrolyte was used.

a)  b) 

Figure 10: Electrolyte injection for (a) Liquid electrolyte with vacuum plunger; (b) Gel electrolyte with syringe

3.1.6 Gel Electrolyte Injection

The vacuum plunger did not work well with the thicker gel electrolyte; therefore a syringe was used. The gel injection process can be observed in Figure 10b, where the cavity is partially filled with electrolyte. Because a syringe was used, two drill holes were needed to provide an air vent and reduce any air bubbles. The gel was prepared by adding 7 wt% of Nanoclay, Nanomer® (1.31PS, montmorillonite clay surface modified with 15-35% octadecylamine and 0.5-5 wt% aminopropyltriethoxysilane, Aldrich) to the liquid electrolyte and using a magnetic stirrer for at least 24 hours to ensure complete dispersion of the nanoclay particles. The resulting gel electrolyte was more viscous, as

seen in Figure 11, but was still thin enough to allow injecting with a standard syringe.

Figure 11: Higher viscosity of gel electrolyte

3.1.7 Sealing Drill Hole

Immediately after the cells were filled with electrolyte, the surface of the glass was dried and the drill holes were sealed with hot glue. While it served the purpose of sealing the hole, the hot glue did not seem to create a strong enough bond with the glass to prevent slow evaporation over time. Glass lids were experimented with, however, the sealant used to affix the lid had to be heated to melt. This was problematic due to the effect on the electrolyte material, and the results did not show a significant improvement. Super glue was attempted as well, but it reacted with the electrolyte causing damage to the cell. This is one part of the process that could still be improved with further research and experimentation with alternative methods. The final product is the DSSC shown in Figure 12.

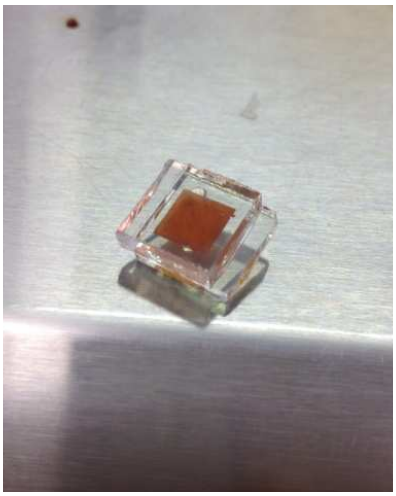

Figure 12: Completed DSSC

3.2 Evaluation of DSSC

The testing setup seen in Figure 13 was comprised of the Oriel 500W Universal Lamp Housing with F/1 (UV grade fused silica collimating condenser) and 152 W Xe OF Arc Lamp (Newport), which was used to simulate the sunlight with AM 1.5. Newport Arc Lamp Power Supply Model 69907 powered the lamp. The I-V curves were obtained using the PARSTAT 2273 Advanced Electrochemical System. The cell was consistently positioned at a height and location under the simulator where it would receive full sun, which is defined as 100 mW/cm^2. The incident light intensity was measured using a daystar meter, which was calibrated using a reference cell from TUV Rheinland PTL (Tempe, AZ). One issue discovered during testing was that pressure from fixed probes making contact with each electrode was causing stress to the sealant and lead to leaks over many testing sessions. Attempts were made to develop an alternate testing station, but reducing pressure consequently reduced

contact with the glass, and therefore, data was affected negatively. The final method used was alligator clips, and caution was taken to reduce any pressure on the electrodes.

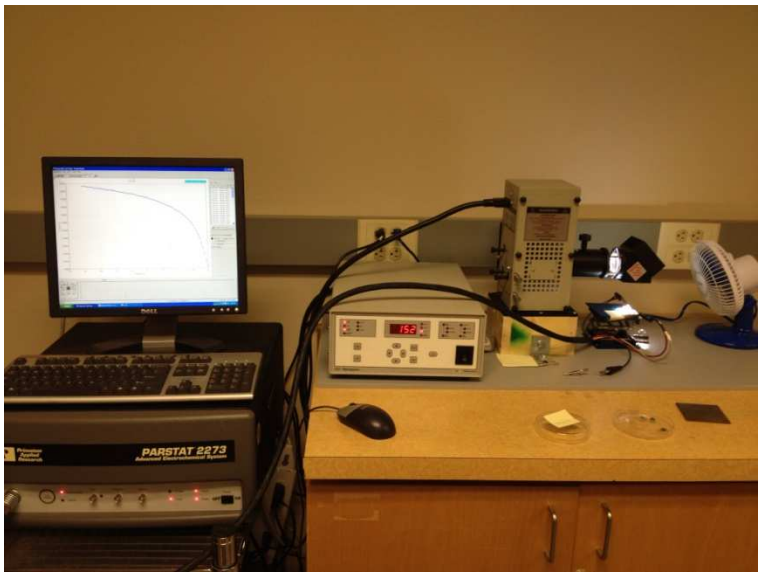

Figure 13: PARSTAT and solar simulator used for testing cells

The PARSTAT testing equipment was set up to sweep the input voltage from V_{OC} to 0 V with a 10 mV interval and the corresponding current at each step was measured. As the voltage decreased to 0 V, the current increased to open circuit current (I_{SC}) forming the I-V curve. In order to reduce the amount of time the cells were under the simulator in order to minimize cell heating, the step time was reduced from 1 sec to 0.065 sec. This change affected the I_{SC} of the curve as the cell degraded, and therefore, further evaluation was performed to determine the ideal step time. When all factors were considered, the decision was made to use a step time of 0.5 sec.

3.3 Intended Research Methods

The experiments conducted in this study were designed to compare a liquid electrolyte DSSC to a similar quasi solid cell created by adding nanoclay particles to the iodide based electrolyte. In order to ensure reliable and consistent data, significant effort was taken to refine the fabrication process and materials used. In addition to the process improvements, the data collection was set up to eliminate as many external variables as possible. Cells were measured at equal intervals, and were exposed to the simulator irradiance for exactly two minutes prior to each measurement. Each batch of four cells was comprised of two liquid and two gel electrolyte cells, so that any fabrication variations between batches would not affect the comparison results. These results are discussed and analyzed in the following chapter.

Chapter 4

RESULTS AND DISCUSSION

4.1 Sample Set

Over the course of this experiment, hundreds of DSSCs were fabricated and tested while the process itself was being refined. Initially, there was an extremely high rate of bad cells, defined as cells with efficiencies less than 1%, being produced. Roughly 65% of the cells coated were successful. After the final experimental method was established, 102 cells were fabricated and tested half with liquid electrolyte and half with nanoclay gel electrolyte. There were a total of 25 bad cells, some of which had been fabricated poorly, others which showed no obvious failures, but had experienced electrolyte loss and were not performing as expected. The latter cells were re-injected with their original electrolyte material in order to assess whether the drill hole had been improperly sealed allowing electrolyte to evaporate, or whether a testing error had occurred. Re-injecting the liquid electrolyte cells was simple and the efficiency measurements taken following the refill were only slightly lower than the initial I-V measurement obtained, but cells with the nanoclay gel electrolyte could not be refilled. The nanoclay electrolyte had hardened inside the cell cavity, which prevented additional injection of material. The total number of bad cells after refilled cells were measured was reduced to 15, leading to a true failure rate of only 14.7%. This was a significant improvement from the initial fabrication results, which showed

that the changes made to the process had in fact improved the quality of cells produced.

4.2 Sealant Issues

One step of the process that was improved upon, but not perfected, was the sealing, which continued to plague the fabrication process throughout the experiment. Even after the hot press replaced the oven as the sealing method, cells that initially showed no signs of leaking gradually began to leak. The leaking became visible after several measurements had been taken, so the frequency of measurements was reduced, and it was determined that storage time was less of a factor, and that the measurement procedure itself was weakening the sealant. When the cells were tested under the solar simulator, the counter electrode was fixed and the weight of the alligator clip attached to the working electrode resulted in a slight force pulling the electrodes apart. The force was not enough to cause any observable effects, but over several applications; the sealant was weakened allowing sealant to penetrate. The quasi-solid cells experienced the same force, but because of the thicker electrolyte, the leakage was minimized, as seen in

, which shows liquid and gel cells from the same batch, which were tested an equal number of times. This observation was a clear indicator of the advantage to using nanoclay gel electrolyte rather than liquid when it comes to minimizing electrolyte loss.

Figure 14: Effects of leakage in liquid and gel cells from the same batch

4.3 Nanoclay Gel Electrolyte

Various gel concentrations were tested in order to find the optimal ratio of nanoclay to liquid electrolyte. Concentrations of 10 wt% had high viscosity, which made fabrication difficult, and concentrations of 5 wt% did not have any significant effect on the viscosity. Concentrations of 7 wt% nanoclay in liquid electrolyte yielded a gel that was more viscous and at the same time thin enough to allow injection with a standard syringe.

4.4 Averaged data

The results obtained from the I-V measurements indicated other advantages exist as well. Overall, the quasi-solid cells outperformed the liquid electrolyte cells in stability, V_{OC}, I_{SC}, and energy conversion efficiency (η). Some cells performed better than other, but this variation is the result of a fabrication process involving many human elements. To normalize the variation, all of the data was compiled and averages for the performance data were calculated and can be seen in Table .

Table 1. Averaged Characteristic Data for All Cells

Electrolyte Type	V_{OC} (V)	I_{SC} (mA/cm^2)	η (%)	Lifetime (days)
Liquid	0.78	12.88	5.19	8.15
Gel	0.82	14.92	5.96	19.96

The most staggering difference observed between liquid and nanoclay gel cells was that the gel cells lasted more than twice as long as their liquid counterparts. On average, the liquid electrolyte cells maintained their initial efficiency for 2-3 days, but that efficiency decreased rapidly to less than 1%, which was used as the minimum efficiency value to be considered as a functioning cell, after 8.15 days. The cells with gel electrolyte maintained initial efficiency longer and showed a slower decrease, resulting in an average lifetime of 19.96 days.

4.5 Calculations

The energy conversion efficiency (η) of the DSSCs was calculated using the fundamental equation,

$$\eta = Output\ Power\ (P_{out}) \div InputPower\ (P_{in})$$

The input power is defined as the intensity of the light on the active cell area,

$$P_{in} = 1000\frac{W}{m^2} \times\ 3.844E^{-05}m^2$$

The active area, 38.44 mm^2, was measured as the area of the cell within the sealant, where the electrolyte material made contact with both

electrodes. 1000 W/m^2 was the intensity of the simulated sunlight from the Oriel simulator.

Output power is equal to the maximum power point (P_{mpp}) calculated by multiply the maximum voltage (V_{max}) and the maximum current (I_{max}), which were obtained from the I-V curve measurements taken for each cell,

$$P_{mpp} = V_{max} \times I_{max}$$

Fill factor (FF) data was calculated using the P_{mpp} and the open circuit voltage (V_{OC}) and short circuit current (I_{SC}) values obtained from the I-V curve measurements,

$$FF = \frac{P_{mpp}}{I_{sc} \cdot V_{oc}}$$

4.6 Comparison of gel and liquid electrolyte cells

In addition to the averaged data shown in Table , Figures 16-19 show the best performing liquid and nanoclay gel cells compared to each other. These two cells lasted the longest within their electrolyte group, and had the highest efficiencies, both greater than 9%. The I-V curves are displayed in Figure 15, which shows that for these cells, the gel electrolyte had a higher maximum ISC, which was generally not the case as seen in the averaged data. Aside from the I_{SC}, the curves are very similar to each other, showing that the gel does not have any noticeable effect on the resistances affecting the DSSCs. The most notable differences occur as the cells age, which is further examined in section 0.

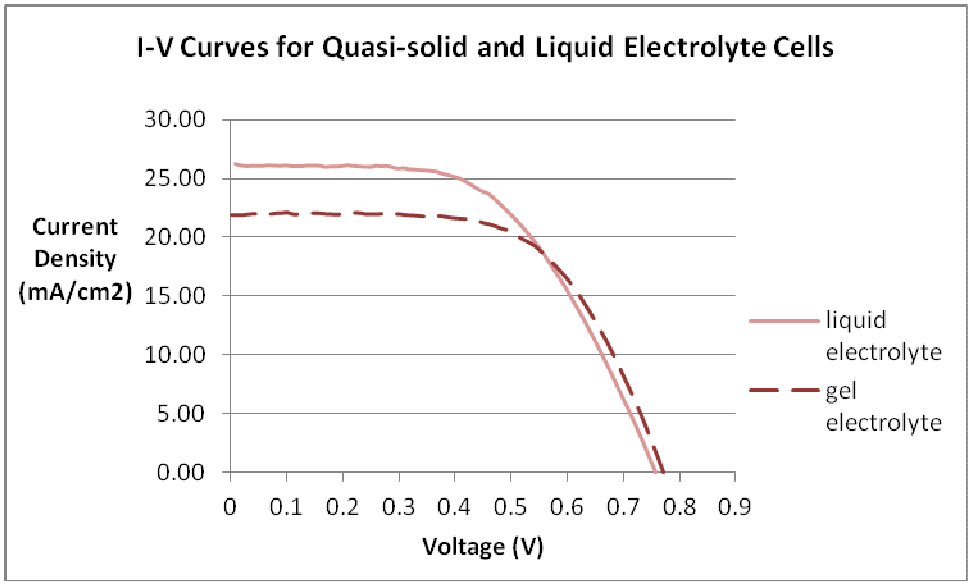

Figure 15: Comparison of I-V curves for liquid and gel electrolyte cells

4.7 Output Characteristics of liquid and gel cells over time

The increase in V_{OC} is illustrated in

Figure 15: Comparison of I-V curves for liquid and gel electrolyte cells, which shows a 9% increase that the liquid electrolyte cell over 10 days compared to the 16% increase from the nanoclay gel electrolyte cell, which took place over 26 days. V_{OC} is the difference between the Fermi level (E_F) of the TiO_2 and the redox potential (I^-/I_3^-) of the electrolyte.

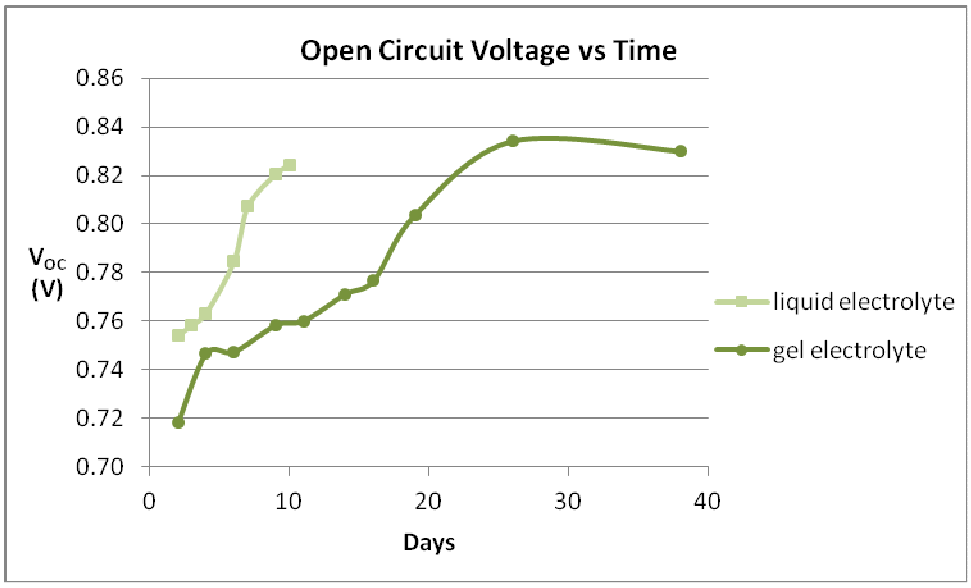

Figure 16: V_{OC} plotted over time for liquid and gel electrolyte cells

The TiO_2 material is consistent between liquid and nanoclay gel cells, so this difference is likely the result of a lower redox potential of the (I^-/I_3^-) when nanoclay is added to the liquid electrolyte.

Figure 17 plots the short circuit current density (I_{SC}/cm^2) over time for both liquid and nanoclay gel cells. Similar to the Voc, the liquid I_{SC} rate of change is much faster than the gel, but the I_{SC} decreases with time instead of increasing like the V_{OC}.

Both cells initially experience a slight increase in I_{SC}, reaching a maximum value of 26.22 mA/cm^2 for the liquid cell, and 23.61 mA/cm^2 for the gel cell, before the steady decline begins. There is also a much greater change with the I_{SC}, which decreases as much as 86% over the lifetime of the cell. This decrease is likely a combination of different factors including electrochemical changes within the cell, but the major contributing factor is the loss of electrolyte that occurs.

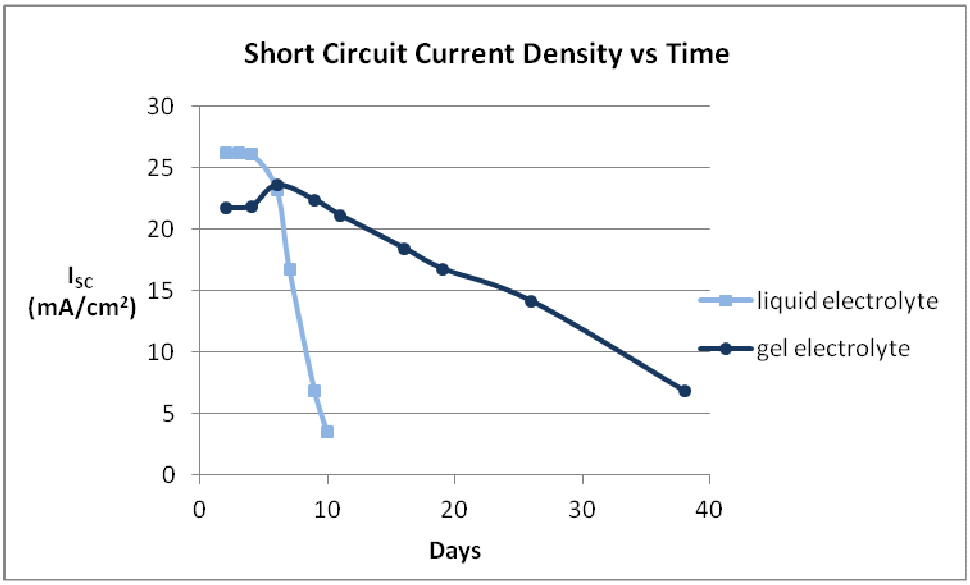

Figure 17: I_{SC} current plotted over time for liquid and gel electrolyte cells

The liquid cells lose electrolyte material faster whether via leakage or evaporation, therefore, their ability to transfer charge carriers decreases, limiting the current. The maximum I_{SC} of the nanoclay gel cell is only slightly less than the best performing liquid electrolyte cell, which combined with the average I_{SC} data in Table , proves that the addition of the nanoclay material does not limit the diffusion of ions.

The energy conversion efficiency follows a similar trend as the I_{SC},

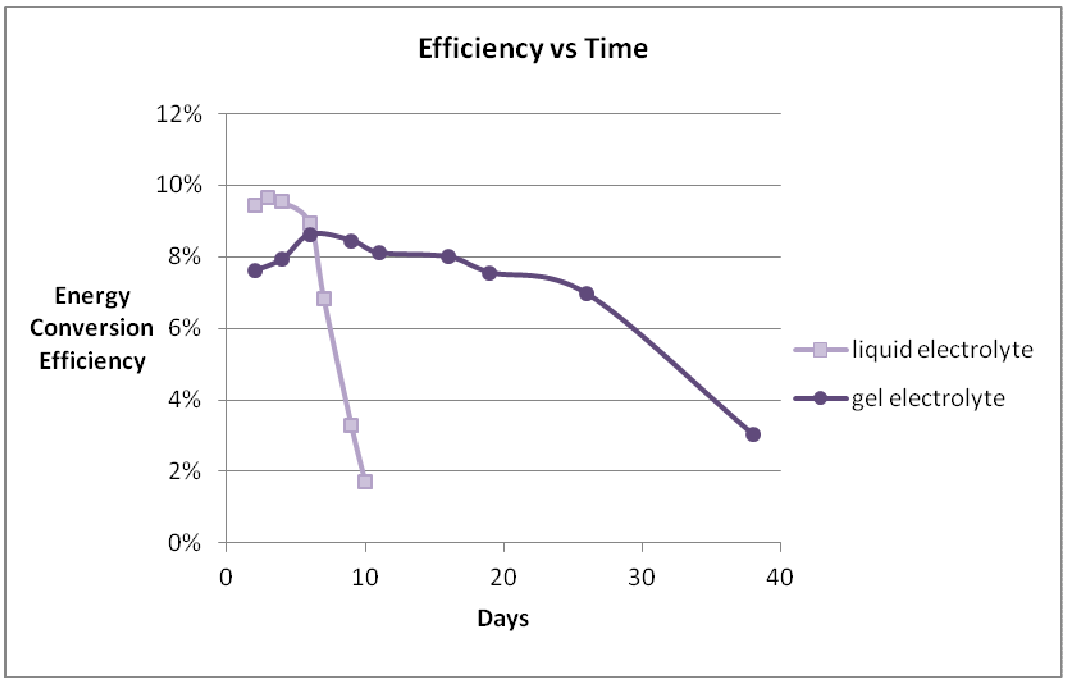

increasing slightly and then steadily decreasing until the cell is dead as shown in Figure 18. The nanoclay gel electrolyte cell maintains a fairly steady efficiency of about 8% for several weeks before steadily declining, which is due to the increase in Voc during this period. While the maximum efficiency of the liquid cell is slightly higher, it is not stable and decreases rapidly.

Figure 18: Conversion efficiency plotted over time for liquid and gel electrolyte cells

4.8 Quasi-solid cell I-V Curve

The I-V curves measured at the beginning, middle, and the end of the gel cell's lifetime are shown in Figure 19. The FF varied slightly, but averaged around 0.61, which was slightly better than the FF of the liquid electrolyte cell. The low FF indicates there were issues with resistance, and based on the shape of the curves shown in Figures 16 and 20, the internal series resistance was the major contributor. However, there was no significant difference between the liquid and gel cells, therefore this was not explored further.

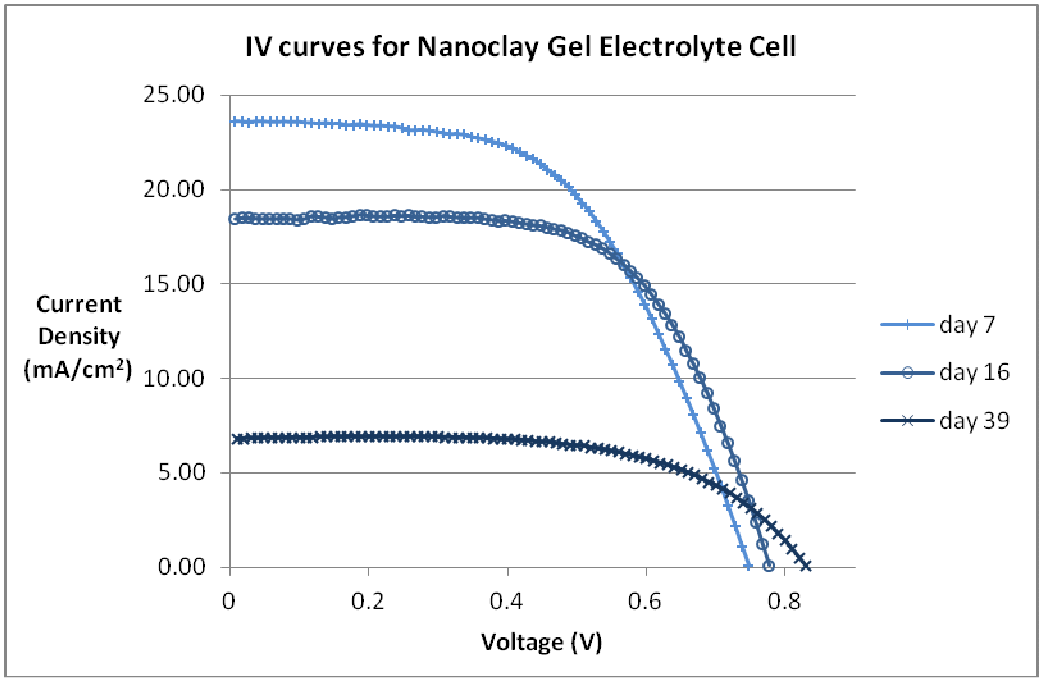

Figure 19: I-V curve progression for nanoclay gel electrolyte cell

Chapter 5 will provide an overview of the conclusions drawn from these experimental results and suggestions for future research opportunities.

Chapter 5

CONCLUSIONS

5.1 Overview

The initial fabrication method being utilized was highly susceptible to human error. This resulted in a high learning curve for the fabrication process, as well as high failure rates. Changes made to the glass substrate cutting, TiO_2 coating process, and final assembly led to a more efficient, repeatable process, with an increased number of working cells fabricated. These improvements made to the existing fabrication lowered the failure rate of production from 65% to only 15%.

The experimental results show that nanoclay is a viable gelator for quasi-solid DSSCs. The addition of nanoclay to an iodide based liquid electrolyte significantly increases stability and also shows a slight improvement of performance characteristics when compared to liquid electrolyte cells with an identical fabrication process. The gel electrolyte that was comprised of 7 wt% nanoclay material showed the best viscosity for existing fabrication procedures.

The average lifetime of a nanoclay gel cell, was more than double that of the liquid electrolyte cells. This significant improvement is due to the nanoclay gel electrolyte's resistance to leakage, which is one of the major setbacks of liquid electrolyte DSSCs. The average V_{OC}, I_{SC}, and energy conversion efficiency results were also higher for the nanoclay gel electrolyte cells, showing that higher viscosity gel electrolyte did not

impede the diffusion of charge carriers. Overall, the quasi-solid cells outperformed the liquid electrolyte cells in all categories evaluated for this experiment.

5.2 Future Recommendations

Leakage into the sealant could be further minimized by improving the test setup so that less pressure is applied to the electrodes. Different sealant material may increase the strength of the bond between electrodes and resist separation during testing.

The ratio of nanoclay to liquid electrolyte can be increased provided other injection methods are employed. A higher viscosity could potentially simplify the fabrication process by eliminating the need for syringe injection and consequently no drilling in the counter electrode would be necessary.

In order to be a viable option for commercialization, the nanoclay gel electrolyte DSSCs need to exhibit stability at high temperatures. High temperature testing was not covered in the scope of this project therefore, that is something that needs to be researched and tested.

In addition to the high temperature testing, more research is needed to develop relevant standardized tests for DSSCs. The cells are based on electrochemical reactions unlike Si based solar cells, and therefore, testing conditions need to reflect these fundamental operational differences. Minor variations in step time resulted in observable differences in I-V measurements. Research is needed to determine the

optimal testing conditions so they can be established as standards for DSSC research and accurately normalize DSSC performance data.

REFERENCES

[1] U.S. Department of Energy, “Domestic Unconventional Fossil Energy Resource Opportunities and Technology Applications Report to Congress”, U.S Department of Energy, Washington, DC, 2011.

[2] Pachauri, R.K and Reisinger, A. (eds.), “Climate Change 2007: Synthesis Report. Contribution of Working Groups I, II and III to the Fourth Assessment Report of the Intergovernmental Panel on Climate Change”, IPCC, Geneva, Switzerland, 2007.

[3] G. Smestad, C. Bignozzi, and R. Argazzi, "Testing of Dye Sensitized TiO2 Solar Cells I: Experimental Photocurrent Output and Conversion Efficiencies", *Solar Energy Materials and Solar Cells*, vol. 32, no. 3, pp. 259-272, 1994.

[4] J. Kalowekamo, and E. Baker, "Estimating the Manufacturing Cost of Purely Organic Solar Cells", *Solar Energy*, vol. 83, no. 8, pp. 1224-1231, 2009.

[5] P. Murray, A. Thein, S. Tulloch, and H. Desilvestro, “Dye solar cells: The new kid on the block”, Dyesol Ltd, & Australia, Q. N, Renewable Energy World [Online]. Available: http://www.renewableenergyworld.com/rea/news/article/2009/05/dye-solar_cells__

[6] B. O'Regan, and M. Grätzel, “A low-cost, high-efficiency solar cell based on dye-sensitized colloidal TiO2 films”, *Nature*, vol. 353, pp. 737-740, Oct 1991.

[7] A. Yella et al., “Porphyrin-sensitized solar cells with cobalt (II/III)–Based redox electrolyte exceed 12 percent efficiency”, *Science*, vol. 334, pp. 629-634, Nov 2011.

[8] A. Hagfeldt, G. Boschloo, L. Sun, L. Kloo, and H. Pettersson, “Dye-sensitized solar cells”, *Chem. Rev.*, vol. 110, pp. 6595-6663, 2010.

[9] D. Kuciauskas, “Electron transfer dynamics in nanocrystalline titanium dioxide solar cells sensitized with ruthenium or osmium polypyridyl complexes”, *The Journal of Physical Chemistry*, vol. 105, pp. 392-403, 2001.

[10] C. Bauer, “Interfacial electron-transfer dynamics in ru(tcterpy)(NCS) - sensitized TiO nanocrystalline solar cells”, *The Journal of Physical Chemistry*, vol. 106, no. 49, pp. 12693-12704, 2002.

[11] D. Bari et al., “Thermal stress effects on dye-sensitized solar cells (DSSCs)”, *Microelectronics Reliability*, vol. 51, no. 9–11, pp. 1762-1766, 2011.

[12] J. Wu, “Progress on the electrolytes for dye-sensitized solar cells”, *Pure and Applied Chemistry*, vol. 80, no. 11, pp 2241-2258, 2008.

[13] N. Cai, “An organic D-π-A dye for record efficiency solid-state sensitized heterojunction solar cells”, *Nano Letters*, vol. 11, no. 4, pp. 1452-1456, 2011.

[14] S. Lu, R. Koeppe, S. Günes, and N. Sariciftci, “Quasi-solid-state dye-sensitized solar cells with cyanoacrylate as electrolyte matrix”, *Solar Energy Materials and Solar Cells*, vol. 91, no. 12, pp. 1081-1086, 2007.

[15] G. Mao, “Relaxation in polymer electrolytes on the nanosecond timescale”, *Nature*, vol. 405, no. 6783, pp. 163-165, 2000.

[16] P. Meneghetti, S. Qutubuddin, and A. Webber, “Synthesis of polymer gel electrolyte with high molecular weight poly(methyl methacrylate)–clay nanocomposite”, *Electrochimica Acta*, vol. 49, no. 27, pp. 4923-4931, 2004.

[17] Q. Yu et al., “A stable and efficient quasi-solid-state dye-sensitized solar cell with a low molecular weight organic gelator”, *Energy Environ.Sci.*, vol. 5, pp. 6151-6155, 2012.

[18] P. Wang, S. Zakeeruddin, P. Comte, I. Exnar, and M. Grätzel, “Gelation of ionic liquid-based electrolytes with silica nanoparticles for quasi-solid-state dye-sensitized solar cells”, *Journal of the American Chemical Society*, vol. 125, no. 5, pp. 1166-1167, 2003.